ChemComm

Accepted Manuscript

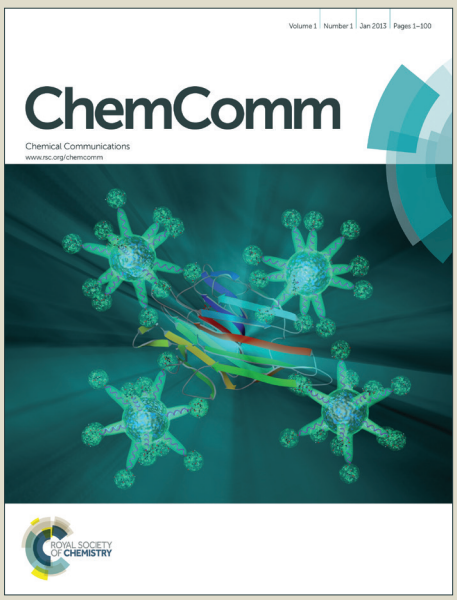

ROYAL SOCIETY OF CHEMISTRY

www.rsc.org/chemcomm

Journal Name

RSCPublishing

COMMUNICATION

A modular designed copolymer with anti-thrombotic activity and imaging capability†

Cite this: DOI: 10.1039/x0xx00000x

Nan Xie,‡[a] Ke Feng,‡[b] Bin Chen,[b] Ming Zhao,*[ac] Li-Ping Zhang,[b] Chen-Ho Tung,[b] Li-Zhu Wu*[b] and Shiqi Peng*[a]

Received 00th January 2012,
Accepted 00th January 2012

DOI: 10.1039/x0xx00000x

www.rsc.org/

Through a modular ROMP (ring-opening metathesis polymerization) strategy, a random copolymer with anti-thrombotic activity and imaging capability has been constructed from RGD, rhodamine B and PEG modified norbornene monomers. As we expected, these tri-component polynorbornenes exhibit significant enhancement in anti-thrombotic efficacy and bioavailability *in vivo*.

Bioactive and functional polymers have attracted an increasing interest for designing intricate architectures in biomedical applications, such as imaging, diagnosis and therapy of disease in the past decades.[1-11] On one hand, varied polymeric structures, like block, random, conjugated, branched and graft polymers, can easily integrate therapeutic agents, imaging labels, targeting ligands, and many other bioresponsive elements for multipurpose functionalities; on the other hand, as a bonus, the multivalent effect[12] and enhanced permeation and retention effect,[13] attributed from the repeat units on the polymer chain, can greatly improve bioavailability and therapeutic efficacy of drugs, increase signal-to-noise ratio for higher imaging quality, and enhance target-binding specificity. However, the design and synthesis of new polymeric candidates in view of their biological implications has just been initiated.[14]

Bioactive peptide sequences including receptor-targeted peptides, nuclear localization signaling peptides (NLSs), cell penetrating peptides (CPPs) and so forth,[15] can act as chemical messengers, neurotransmitters, agonists or antagonists against specific receptors to regulate many critical life processes, whose incorporation would endow the polymeric structures or architectures with therapeutic or targeted functions.[3] RGD (arginine-glycine-aspartic acid) sequence as one of the typical receptor-targeted peptides, binds to integrins with high specificity and affinity, plays important roles in a series of physiological and pathological processes by mediating cell-extracellular matrix (ECM) or cell-cell interactions, and thereby is the most common target for therapeutic and diagnostic purpose. For instance, RGD peptides have been shown to have anti-thrombotic activity by inhibiting the fibrinogen binding to the integrin glycoprotein GPIIb/IIIa receptor and blocking the pathway that leads to platelet aggregation and subsequent thrombus formation, thus may be good prospects for thrombosis treatment.[16]

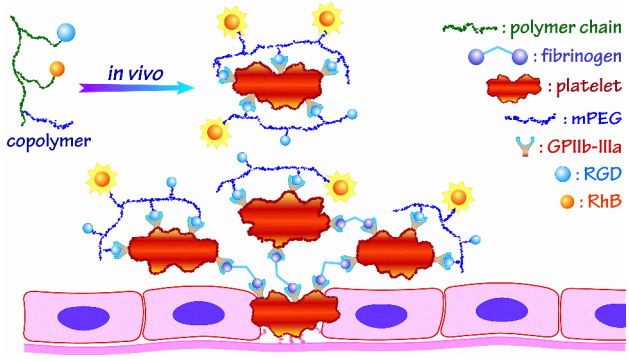

Scheme 1 Design of RGD-modified copolymers for targeting GPIIb/IIIa receptor on activated platelets involved in thrombotic events.

Ring-opening metathesis polymerization (ROMP) initiated by ruthenium *N*-heterocyclic carbene complexes is a powerful toolkit for the preparation of random, block and alternating functionalized copolymers from cyclic olefin backbones with well-controlled molecular weight, narrow polydispersity indices (PDIs) and special duration to certain function groups.[17-26] Grubbs and co-workers synthesized biofunctionalized polynorbornenes by ROMP directly from RGD monomers and prepared thin films with enhanced cell adhesive properties.[18c,d] In particular, ROMP-derived polymers with polynorbornene backbones have been proved to be nontoxic in a variety of biological systems.[25] Inspired by this work, we developed a modular strategy[27] to fabricate random copolymers through a simple one-pot multi-component ROMP. Herein, a water-soluble copolymeric material was designed and constructed in the present work, integrating anti-thrombotic activity and thrombus imaging capability from designable norbornene monomers. To tailor the therapeutic and imaging functions, these copolymers were equipped with RGD sequence for a therapeutic purpose owing to its anti-thrombotic activity (Scheme 1), poly(ethylene glycol) (PEG) units as a hydrophilic solubilizer, and rhodamine B (RhB) dye as fluorescence reporter for thrombus imaging because they possess a set of distinguished properties of bioorthogonality, good photostability, high extinction coefficients and fluorescence quantum

yield, which are crucial advantages for long-term sensitive fluorescence applications.[28]

Our studies commenced with the preparation of peptide module, the fully protected RGD norbornene monomer was readily obtained by standard Fmoc solid phase peptide synthesis (SPPS) on 2-chlorotrityl chloride resin. After step-by-step introduction of protected S, D, G and R units, norbornenyl carboxylic acid was used as the last unit to terminate the peptide sequence. In the meantime, a soft spacer, 6-aminohexanoic acid, was incorporated between the highly functionalized RGDS peptide sequence and the ROMP reactive norbornene, which will enhance the molecular flexibility of the RGD monomer and improve its reactivity during polymerization. Cleavage from resin in an acidic condition directly gave the side-chain fully protected RGD peptide monomer, it was well characterized by NMR, MS and EA, and can be subjected to the subsequent copolymerization without any need for further purification. Beyond RGD, the norbornene-acid-terminated SPPS also provided a quick and easy solution for the preparation of diverse peptide norbornene monomers with desirable and designable sequence. Homopolymerization from peptide monomers can be achieved in couples of solvents, such as $CHCl_3$, CH_2Cl_2, CH_3OH, THF and so on,[18c,d,22] but it was still hampered by undesirable physicochemical problems including uncontrollable polymeric molecular weights and polydispersity indices (PDIs) as well as limited solubility in processible solvents, which originate from intermolecular hydrophobic aggregation of the protected peptide chains or the formation of assembly structures.[29] To overcome these deficiencies, PEG was designed as a hydrophilic module during copolymerization, which is widespread in pharmaceutical and biomedical industry. PEG modification (PEGylation) of peptides, proteins, liposomes, dendrimers, and various biomaterials has been shown to significantly increase the water solubility, on one hand, and reduce the antigenicity and immunogenicity maintaining bioactivity and biocompatibility *in vivo*, on the other hand.[30] The PEG monomer was readily synthesized by esterification between norbornenyl carboxylic acid and methoxypolyethylene glycol-350 (mPEG-350). MS spectrum confirmed each component of obtained NB-$COO(CH_2CH_2O)_nCH_3$ (n = 7~14), which is well fit to a normal distribution in amount. Rhodamine B monomer was prepared analogously from alcohol norbornene precursor, and acted as a chromophore module to endow the copolymer with fluorescent imaging capability. In addition, other functionlized norbornene monomers can also be derived from carboxyl, hydroxyl and amino precursors *via* esterification or amidation. The modular ROMP strategy enables the fabrication of multifunctional polynobornenes from varied function monomers, and provides a diversity of biomedical applications, such as subcellular imaging, tissue-specific diagnosis and targeting therapy through peptide sequence permutations and chromophore modifications from our ongoing constructed libraries.

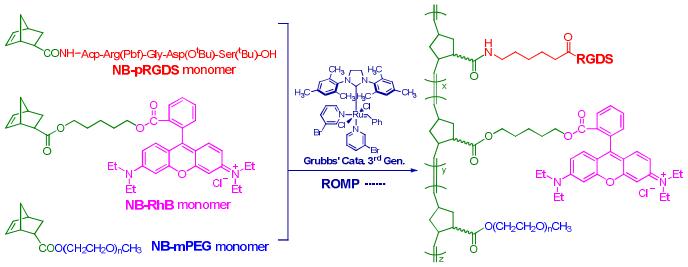

Fig. 1 The preparation of PNB-$RGDS_x$-*co*-RhB_y-*co*-$mPEG_z$ random copolymers.

As illustrated in Fig. 1, copolymer PNB-$pRGDS_x$-*co*-RhB_y-*co*-$mPEG_z$ were prepared empirically from suitable feeding proportions of RGD monomer (NB-pRGDS), Rhodamine B monomer (NB-RhB) and PEG monomer (NB-mPEG) *via* ROMP by initiation with Grubbs' third-generation catalyst in $CHCl_3$. The homopolymerization for PEG monomer was firstly investigated, a linear dependence of average molecular weights (M_n) of these polymers on different monomer-to-catalyst ratios [M]/[C] of 25:1, 50:1, 75:1, and 100:1 indicated a living characteristics during ROMP (Fig. S2, ESI†). Simultaneously, ^{1}H NMR spectra (Fig. S3, ESI†) showed complete disappearance of the carbene signal of the initiator at 19.1 ppm, accompanied by the formation of two new broad carbene signals at 18.5 and 18.3 ppm. As a degree of polymerization (DP) was fixed at 100 (*i.e.* the molar ratio of total feeding amounts of monomers to Grubbs' third-generation initiator was 100:1), the NB-pRGDS proportion x varied from 0 to 15, the NB-RhB proportion y was held constant at 5, and the NB-mPEG was incorporated as needed to keep the ratio of monomers to catalyst constant. The GPC data listed as Table 1, the PDIs of the resulting PNB-$pRGDS_x$-*co*-RhB_y-*co*-$mPEG_z$ copolymers were relatively narrow (1.17~1.38), and the molecular weight of M_n was in the range of 45~58 kDa, which showed a reasonable relationship with the total feeding amounts of the monomers. The inclusion of a soft spacer (6-aminohexanoic acid) made the strained polynorbornene backbones more flexible and reduced the aggregation and steric hindrance of the peptide branches, resulting in the complete consumption of feeding monomers and the generation of polymers with narrow PDIs during random copolymerization.

Table 1 GPC data for PNB-$pRGDS_x$-*co*-RhB_y-*co*-$mPEG_z$ and PNB-$RGDS_x$-*co*-RhB_y-*co*-$mPEG_z$ random copolymers.

Polymer[a)]	M_n [kDa]	M_w [kDa]	PDI
PNB-$pRGDS_{10}$-*co*-$mPEG_{90}$	57.6	69.3	1.20
PNB-$RGDS_{10}$-*co*-$mPEG_{90}$	50.6	60.1	1.19
PNB-RhB_5-*co*-$mPEG_{95}$	44.7	57.2	1.28
PNB-$pRGDS_5$-*co*-RhB_5-*co*-$mPEG_{90}$	46.5	54.2	1.17
PNB-$pRGDS_{10}$-*co*-RhB_5-*co*-$mPEG_{85}$	56.8	73.3	1.29
PNB-$pRGDS_{15}$-*co*-RhB_5-*co*-$mPEG_{80}$	52.0	71.8	1.38
PNB-$RGDS_5$-*co*-RhB_5-*co*-$mPEG_{90}$	45.1	52.6	1.17
PNB-$RGDS_{10}$-*co*-RhB_5-*co*-$mPEG_{85}$	51.4	65.9	1.28
PNB-$RGDS_{15}$-*co*-RhB_5-*co*-$mPEG_{80}$	49.4	67.3	1.36

[a)] Measured in DMF with 25 mM LiBr at 313 K.

The side-chain protecting groups of the PNB-$pRGDS_x$-*co*-RhB_y-*co*-$mPEG_z$ copolymers were cleaved with a mixture of 95% TFA, 2.5% H_2O and 2.5% triisopropylsilane. After counterion exchange with NaCl and dialysis in refrigerator, the deprotected PNB-$RGDS_x$-*co*-RhB_y-*co*-$mPEG_z$ copolymers were yielded as red solids after lyophilization. The removal of protecting groups can be monitored by ^{1}H NMR. The spectrum of copolymer PNB-$pRGDS_{10}$-*co*-RhB_5-*co*-$mPEG_{85}$ (Fig. S28 in ESI†) resembles a stoichiometric superposition of its components of PNB-pRGDS, PNB-RhB and PNB-mPEG homopolymers (Fig. S17, 21 and 24 in ESI†). Compared with the spectrum after cleavage (Fig. S29 in ESI†), the disappearance of three single peaks at 1.03, 1.32 and 1.38 ppm, corresponding to *t*-butyl, *t*-butoxy and 2,2,4,6,7-pentamethyldihydrobenzofuran-5-sulfonyl (Pbf) protecting groups, respectively, ensures the complete removal of side-chain protecting groups after treatment with TFA. Furthermore, GPC measurements verified the decrease in molecular weights as well as the comparable PDIs, shown as Table 1.

Since fluorescent imaging is one of our important motivations, the photophysical properties of PNB-$RGDS_x$-*co*-RhB_y-*co*-$mPEG_z$ copolymers as well as NB-RhB monomer were carefully studied in physiological solution. As shown in Fig. S4 in ESI†, both of the

copolymer and monomer exhibit the same characteristic shapes in UV-Vis absorption spectra with a strong absorption band at 561 nm, corresponding to the typical rhodamine B chromophore. While the absorbance from RGD and PEG units were negligible in the near ultra-violet or visible region. The fluorescence of PNB-RGDS$_{10}$-*co*-RhB$_5$-*co*-mPEG$_{85}$ was given as the black curve with a maximum emission peak at 592 nm and a lifetime of 1.66 ns (Fig. S7, ESI†), which was almost identical with that of NB-RhB monomer with a maximum emission peak at 590 nm and a lifetime of 1.60 ns (Fig. S6, ESI†).

The PNB-RGDS$_x$-*co*-RhB$_y$-*co*-mPEG$_z$ copolymer was employed as an anti-thrombotic agent and evaluated in a rat model of artery-vein bypass thrombosis. In this *in vivo* assay, the optimized PNB-RGDS$_{10}$-*co*-mPEG$_{90}$ copolymer was administrated orally, while aspirin, normal saline (NS) and RGD monomer were used as positive control, negative control and reference groups, respectively, then the thrombus formed in treated rats were weighed. The histograms were given as Fig. 2. The RGD monomer showed no obviously anti-thrombotic activities at low concentration, its effective dosage was as high as 5.0 μmol/kg. On the same level thrombosis inhibition in the treated rats, the value for RGD copolymer was only at a dose of 15 nmol/kg. Linear regression analyses suggested that the efficacy of copolymer is 430-folds higher than that of RGD monomer. Control experiment performed in the absence of RGD module, the PNB-mPEG homopolymer exhibited no anti-thrombotic activity at the comparative doses. It implies that activated RGD peptides play a crucial role in our *in vivo* anti-thrombosis. The greatly enhanced efficacy of PNB-RGDS$_{10}$-*co*-mPEG$_{90}$ copolymer was attributed to the covalent modification of RGD module on the polynorbornene scaffold, which suppresses enzymatic degradation, increases systemic absorption, and improves the bioavailability after oral administration.[31]

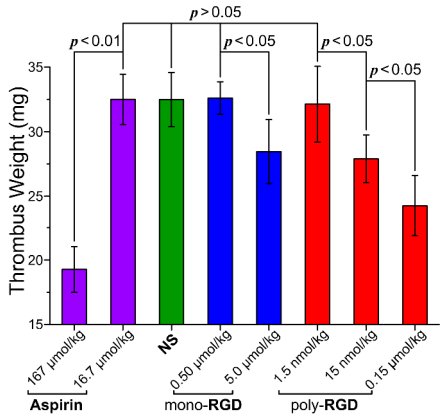

Fig. 2 Dose-dependent anti-thrombotic activity (n = 10) of PNB-RGDS$_{10}$-*co*-mPEG$_{90}$. Thrombus weight of the treated rat is represented as mean ± SD mg, NS = normal saline.

Clot fluorescence experiments were subsequently carried out with the aid of RhB module, the tri-component PNB-RGDS$_x$-*co*-RhB$_y$-*co*-mPEG$_z$ polymers would target the pre-prepared thrombus through the GPIIb/IIIa receptors on the surface of activated platelets. For quantitative comparison, the doping rate for RhB module was held constant at 5. After incubation with individual copolymers with varied RGD contents, the reflectance fluorescence intensities of the clots were measured at 592 nm to evaluate the thrombus binding activities. As shown as Fig. 3a-d, the fluorescence intensities at given instrumental configuration for PNB-RGDS$_x$-*co*-RhB$_5$-*co*-mPEG$_{95-x}$ (x = 0, 5, 10 and 15) copolymers presented a RGD-dependent manner. All RGD containing copolymers exhibited much stronger fluorescence than the PNB-RhB$_5$-*co*-mPEG$_{95}$ reference. Typically, clots incubated with PNB-RGDS$_{10}$-*co*-RhB$_5$-*co*-mPEG$_{85}$ showed a 5.4-folds fluorescence enhancement in comparison with that of PNB-RhB$_5$-*co*-mPEG$_{95}$. In addition, the decay profile of RhB fluorescence for the PNB-RGDS$_{10}$-*co*-RhB$_5$-*co*-mPEG$_{85}$ copolymer after incubation with clot gave the lifetime of 1.45 ns (Fig. S8, ESI†). The obviously shortened lifetime demonstrated that the clot binding indeed takes place between the GPIIb/IIIa receptor and the active RGD module on the copolymers. The binding specificity of target receptor was further confirmed by the competitive assays. As fluorescent PNB-RGDS$_{10}$-*co*-RhB$_5$-*co*-mPEG$_{85}$ copolymer was added as a competitor to the pre-incubated clots with non-fluorescent PNB-RGDS$_{10}$-*co*-mPEG$_{90}$ copolymer or RGD monomer (Fig. 3e-g), the great difference in fluorescence enhancement gave unambiguous evidence that the modular designed PNB-RGDS$_x$-*co*-RhB$_y$-*co*-mPEG$_z$ polymers, for bearing repeating RGD units on the backbones, exhibit much greater binding affinity to the GPIIb/IIIa receptor on the clot than the RGD monomer. Moreover, fluorescent PNB-RGDS$_{10}$-*co*-RhB$_5$-*co*-mPEG$_{85}$ copolymer presented desired thrombus imaging capability as shown as Fig. S9 (ESI†). Given these features, the validated copolymer may prove to be a valuable asset in investigations that aim to track and quantify thrombosis *in vivo*.

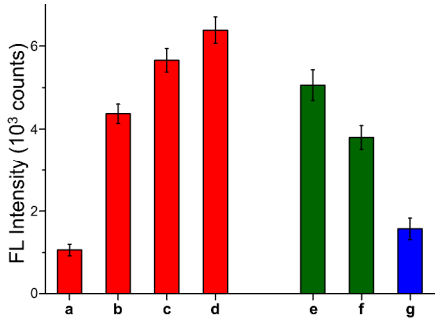

Fig. 3 *In vitro* binding assay of compolymers to thrombi (n = 5). (a-d) Binding activities of non-RGD polymer and a range of 5-15% RGD containing copolymers. (e-g) Competitive banding studies of non-fluorescent RGD-modified copolymer and RGD monomer. a) PNB-RhB$_5$-co-mPEG$_{95}$; b) PNB-RGDS$_5$-co-RhB$_5$-co-mPEG$_{90}$; c) PNB-RGDS$_{10}$-co-RhB$_5$-co-mPEG$_{85}$; d) PNB-RGDS$_{15}$-co-RhB$_5$-co-mPEG$_{80}$; e) 1-fold mono-RGD + PNB-RGDS$_{10}$-co-RhB$_5$-co-mPEG$_{85}$; f) 10-fold mono-RGD + PNB-RGDS$_{10}$-co-RhB$_5$-co-mPEG$_{85}$; g) PNB-RGDS$_{10}$-co-mPEG$_{90}$ + PNB-RGDS$_{10}$-co-RhB$_5$-co-mPEG$_{85}$.

In conclusion, we have constructed a water-soluble polymeric material with anti-thrombotic activity and thrombus imaging capability *via* a simple one-pot multi-component ROMP. To tailor the multi-functions, these copolymers were equipped with the RGD peptide sequence as an anti-thrombotic module for targeting glycoprotein GPIIb/IIIa receptor on the activated platelets, the rhodamine B dye as a reporter module for fluorescence imaging, and the PEG solubilizer as a hydrophilic module for improving biocompatibility. Attributed from the repeating units on the backbones, these tri-component copolymers exhibit significant enhancement in anti-thrombotic efficacy and bioavailability *in vivo*. Importantly, the modular ROMP is verified as a flexible and powerful strategy to fabricate polynobornenes from varied function monomers, and provides a diversity of biomedical applications, such as subcellular imaging, tissue-specific diagnosis and targeting therapy through peptide sequence permutations and chromophore modifications from our ongoing constructed libraries.

We are grateful to Beijing Area Major Laboratory of Peptide and Small Molecular Drugs, the Ministry of Science and Technology of China (2013CB834505 and 2014CB239402), the NSFC (21204052, 21372232 and 91027041), Beijing Municipal Education Commission

Science & Technology (KM201110025003), Solar Energy Initiative of the Knowledge Innovation Program of CAS, and the Foundation of Director of TIPC for financial support.

Notes and references

[a] School of Chemical Biology and Pharmaceutical Sciences, Capital Medical University, Beijing 100069, P. R. China. E-mail: mingzhao@bjmu.edu.cn; sqpeng@bjmu.edu.cn

[b] Key Laboratory of Photochemical Conversion and Optoelectronic Materials, Technical Institute of Physics and Chemistry, The Chinese Academy of Sciences, Beijing 100190, P. R. China. E-mail: lzwu@mail.ipc.ac.cn

[c] Department of Biomedical Science and Environmental Biology, Kaohsiung Medical University, Kaohsiung, Taiwan.

† Electronic Supplementary Information (ESI) available: detailed experimental procedures, supplementary results and figures. See DOI: 10.1039/c000000x/

‡ Equal contribution.

1 M. Elsabahy and K. L. Wooley, *Chem. Soc. Rev.*, 2012, **41**, 2545.

2 L. A. Canalle, D. W. P. M. Lowik and J. C. M. van Hest, *Chem. Soc. Rev.*, 2010, **39**, 329.

3 J. Nicolas, S. Mura, D. Brambilla, N. Mackiewicz and P. Couvreur, *Chem. Soc. Rev.*, 2013, **42**, 1147.

4 C. Zhu, L. Liu, Q. Yang, F. Lv and S. Wang, *Chem. Rev.*, 2012, **112**, 4687.

5 K.-Y. Pu and B. Liu, *Adv. Funct. Mater.*, 2011, **21**, 3408.

6 Z. Ge and S. Liu, *Chem. Soc. Rev.*, 2013, **42**, 7289.

7 Q. Yin, F. Y. Yap, L. Yin, L. Ma, Q. Zhou, L. W. Dobrucki, T. M. Fan, R. C. Gaba and J. Cheng, *J. Am. Chem. Soc.*, 2013, **135**, 13620.

8 Q. Yan and Y. Zhao, *J. Am. Chem. Soc.*, 2013, **135**, 16300.

9 R. Cheng, F. Meng, C. Deng, H.-A. Klok and Z. Zhong, *Biomaterials*, 2013, **34**, 3647.

10 C.-Y. Chen, T. H. Kim, W.-C. Wu, C.-M. Huang, H. Wei, C. W. Mount, Y. Tian, S.-H. Jang, S. H. Pun and A. K. Y. Jen, *Biomaterials*, 2013, **34**, 4501.

11 W. Sun, J. Yu, R. Deng, Y. Rong, B. Fujimoto, C. Wu, H. Zhang and D. T. Chiu, *Angew. Chem., Int. Ed.*, 2013, **52**, 11294-11297.

12 U. Boas and P. M. H. Heegaard, *Chem. Soc. Rev.*, 2004, **33**, 43.

13 (a) D. F. Baban and L. W. Seymour, *Adv. Drug Deliv. Rev.*, 1998, **34**, 109; (b) H. Maeda, J. Wu, T. Sawa, Y. Matsumura and K. Hori, *J. Controlled Release*, 2000, **65**, 271; (c) A. K. Iyer, G. Khaled, J. Fang and H. Maeda, *Drug Discov. Today*, 2006, **11**, 812.

14 J. Khandarea and T. Minko, *Prog. Polym. Sci.*, 2006, **31**, 359.

15 (a) S. Lee, J. Xie and X. Chen, *Biochemistry* 2010, **49**, 1364; (b) K. M. Stewart, K. L. Horton and S. O. Kelley, *Org. Biomol. Chem.*, 2008, **6**, 2242.

16 (a) C. S. Cierniewski, T. Byzova, M. Papierak, T. A. Haas, J. Niewiarowska, L. Zhang, M. Cieslak and E. F. Plow, *J. Biol. Chem.*, 1999, **274**, 16923; (b) R. Pytela, M. Pierschbacher, M. Ginsberg, E. Plow and E. Ruoslahti, *Science*, 1986, **231**, 1559; (c) F. D. Suvire, A. M. Rodríguez, M. L. Mak, J. G. Papp and R. D. Enriz, *J. Mol. Struc.-Theochem*, 2001, **540**, 257; (d) A. McNicol and S. J. Israels, *J. Pharmacol. Sci.*, 2003, **93**, 381; (e) Y.-X. Li, Q. Sun, H. Zhang, S.-T. Ren, Y.-R. Liao, Y. Wang, X.-L. Shen and B. Wang, *Thromb. Res.*, 2012, **129**, e217.

17 A. Fürstner, *Angew. Chem., Int. Ed.*, 2000, **39**, 3012.

18 (a) T. M. Trnka and R. H. Grubbs, *Acc. Chem. Res.*, 2000, **34**, 18; (b) J. A. Love, J. P. Morgan, T. M. Trnka and R. H. Grubbs, *Angew. Chem., Int. Ed.*, 2002, **41**, 4035; (c) R. M. Conrad and R. H. Grubbs, *Angew. Chem. Int. Ed.*, 2009, **48**, 8328; (d) P. R. Patel, R. C. Kiser, Y. Y. Lu, E. Fong, W. C. Ho, D. A. Tirrell and R. H. Grubbs, *Biomacromolecules*, 2012, **13**, 2546.

19 U. Drechsler, R. J. Thibault and V. M. Rotello, *Macromolecules*, 2002, **35**, 9621.

20 S. K. Yang, A. V. Ambade and M. Weck, *Chem. Soc. Rev.*, 2011, **40**, 129.

21 (a) A. Leitgeb, J. Wappel and C. Slugovc, *Polymer*, 2010, **51**, 2927; (b) M. Sandholzer, A. Lex, G. Trimmel, R. Saf, F. Stelzer and C. Slugovc, *J. Polym. Sci. Part A: Polym. Chem.*, 2007, **45**, 1336.

22 K. S. Roberts and N. S. Sampson, *J. Org. Chem.*, 2003, **68**, 2020.

23 E. J. Foster, E. B. Berda and E. W. Meijer, *J. Am. Chem. Soc.*, 2009, **131**, 6964.

24 K. Lienkamp, A. E. Madkour, A. Musante, C. F. Nelson, K. Nüsslein and G. N. Tew, *J. Am. Chem. Soc.*, 2008, **130**, 9836.

25 E. M. Kolonko, J. K. Pontrello, S. L. Mangold and L. L. Kiessling, *J. Am. Chem. Soc.*, 2009, **131**, 7327.

26 (a) K. Vehlow, D. Wang, M. R. Buchmeiser and S. Blechert, *Angew. Chem., Int. Ed.*, 2008, **47**, 2615; (b) D. Le, V. Montembault, J. C. Soutif, M. Rutnakornpituk and L. Fontaine, *Macromolecules*, 2010, **43**, 5611; (c) N. B. Sankaran, A. Z. Rys, R. Nassif, M. K. Nayak, K. Metera, B. Chen, H. S. Bazzi and H. F. Sleiman, *Macromolecules*, 2010, **43**, 5530; (d) S. C. G. Biagini and A. L. Parry, *J. Polym. Sci., Part A: Polym. Chem.*, 2007, **45**, 3178; (e) F. Gueugnon, I. Denis, D. Pouliquen, F. Collette, R. Delatouche, V. Héroguez, M. Grégoire, P. Bertrand and C. Blanquart, *Biomacromolecules*, 2013, **14**, 2396.

27 (a) K. Feng, N. Xie, B. Chen, L.-P. Zhang, C.-H. Tung and L.-Z. Wu, *Macromolecules*, 2012, **45**, 5596; (b) N. Xie, K. Feng, B. Chen, M. Zhao, S. Peng, L.-P. Zhang, C.-H. Tung and L.-Z. Wu, *J. Mater. Chem. B*, 2014, **2**, 502.

28 M. Fernandez-Suarez and A. Y. Ting, *Nat. Rev. Mol. Cell Biol.*, 2008, **9**, 929.

29 T. Wöhr, F. Wahl, A. Nefzi, B. Rohwedder, T. Sato, X. Sun and M. Mutter, *J. Am. Chem. Soc.*, 1996, **118**, 9218.

30 J. M. Harris and R. B. Chess, *Nat. Rev. Drug Discov.*, 2003, **2**, 214-221.

31 T. M. Allen and P. R. Cullis, *Science*, 2004, **303**, 1818.

